CHEMISTRY
A European Journal

A Journal of
ChemPubSoc Europe

Accepted Article

Title: The Cyclopropyl Group: An Excited State Aromaticity Indicator?

Authors: Rabia Ayub, Raffaello Papadakis, Kjell Jorner, Burkhard Zietz, and Henrik Ottosson

To be cited as: *Chem. Eur. J.* 10.1002/chem.201701404

Link to VoR: http://dx.doi.org/10.1002/chem.201701404

Supported by
ACES

WILEY-VCH

10.1002/chem.201701404

The Cyclopropyl Group: An Excited State Aromaticity Indicator?

Rabia Ayub [†‡], Raffaello Papadakis[†‡], Kjell Jorner[†‡], Burkhard Zietz,[‡] and Henrik Ottosson[†‡]*

[†] Department of Chemistry - BMC, Uppsala University, Box 576, 751 23 Uppsala, Sweden.

[‡] Department of Chemistry - Ångström Laboratory Uppsala University, Box 523, 751 20 Uppsala, Sweden.

Abstract: The cyclopropyl (cPr) group, a well-known probe for radical character at atoms to which it is connected, is tested as an indicator for aromaticity in the first ππ* triplet and singlet excited states (T_1 and S_1). Baird's rule tells that the π-electron counts for aromaticity and antiaromaticity in the T_1 and S_1 states are opposite to Hückel's rule in the ground state (S_0). Our hypothesis is that the cPr group, as a result of Baird's rule, will remain closed when attached to an excited state aromatic ring, enabling it to be used as an indicator to distinguish excited state aromatic rings from excited state antiaromatic and nonaromatic ones. Quantum chemical calculations and photoreactivity experiments support our hypothesis; calculated aromaticity indices reveal that openings of cPr substituents on [4*n*]annulenes ruin the excited state aromaticity in energetically unfavorable processes. Yet, polycyclic compounds influenced by excited state aromaticity (*e.g.*, biphenylene), as well as 4*n*π-electron heterocycles with two or more heteroatoms represent limitations.

10.1002/chem.201701404

TOC image

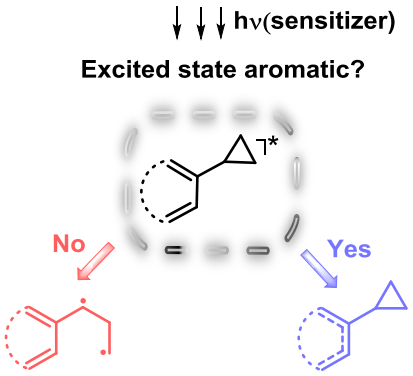

Introduction

Is there a fundamental difference in the photoreactivities of [4*n*+2]- and [4*n*]annulenes? In their electronic ground states (S_0) annulenes with 4*n*+2 and 4*n* π-electrons have drastically different reactivities; benzene is exceptionally reluctant to break up its aromatic cycle while cyclobutadiene (CBD) and cyclooctatetraene (COT) either very rapidly or readily undergo a range of reactions.[1] If there is also a large reactivity difference between [4*n*+2]- and [4*n*]annulenes in their excited states, how can it be explained?

The excited state (anti)aromaticity (ES(A)A) concept has recently gained increased attention,[2,3] although it was first applied in the mid-60s by Dewar and Zimmerman to rationalize allowed and forbidden pericyclic reactions (both thermal and photochemical) in terms of transition state aromaticity and antiaromaticity, respectively.[4,5] The usage of the concept to structures that are minima on excited state surfaces stems from 1972 when Baird used perturbation molecular orbital theory to show that [4*n*+2]annulenes are antiaromatic in their lowest ππ* triplet states (T_1) while [4*n*]annulenes are aromatic.[6,7] Today, Baird's rule has been confirmed through numerous quantum chemical studies,[2] and it has been found to also apply to the lowest singlet excited state (S_1) of small annulenes.[8-11]

Wan and co-workers pioneered the usage of excited state aromaticity (ESA) in an experimental context by concluding that the driving force for photolysis of fluoren-9-ol is the formation of an aromatic 4π cationic species in the excited state.[12] Ottosson, Kilså, and co-workers showed experimentally that the ES(A)A concept can be used to rationalize substituent related variations in the excitation energies of the T_1 and S_1 states of various fulvenes.[13] Recently, explicit spectroscopic evidence for Baird's rule in the excited states was given by Kim, Osuka and co-workers who investigated [26]- and [28]hexaphyrins known to be, respectively, aromatic and antiaromatic in their S_0 states.[14,15]

Based on Baird's rule one can conclude that excited state antiaromatic [4*n*+2]annulenes will photoreact rapidly while [4*n*]annulenes should be photochemically inert and resemble [4*n*+2]annulenes in their S_0 states. Indeed, the excited state antiaromatic character of the benzene ring can be used to identify and develop new photoreactions,[16,17] and one can apply the ES(A)A concept to reanalyze a series of earlier findings.[2] *E.g.*, Paquette and co-workers observed that 1,2-dialkylcyclooctatetraenes are photostable in acetone solution since only starting material was recovered after 100 hours of irradiation,[18] a photostability in line with T_1 aromaticity. Indeed, computational studies have revealed that T_1 aromaticity goes with energy gain and the opposite for T_1 antiaromaticity.[19-21] Now, is there a structural moiety that indicates whether a molecule is aromatic, or not, in its T_1 and S_1 states?

The cyclopropyl (cPr) group indicates radical character by ring-opening when attached to a radical center (Scheme 1),[22] and also when attached to singlet and triplet diradicals.[23,24] The rate of ring-opening of the cyclopropylcarbinyl radical (**1**) is 6.7 x 10^7 s^{-1}, corresponding to a lifetime of 14.9 ns, and the reaction leads to the 3-butenyl radical.[25-27] The calculated activation and reaction free energies for ring-opening of **1** at CBS-RAD level are 7.2 and -3.0 kcal/mol, respectively,[28] while the experimentally reported activation energy

is 5.9 kcal/mol.[29,30] Moreover, gas phase photolysis studies of cyclopropylbenzene performed both with λ = 214 and 254 nm irradiation have revealed that the C_α-C_β bond of the cPr group is highly photolabile.[31,32] Yet, we argue that it will remain closed when attached to a [4*n*]annulene stabilized by aromaticity in its T_1 state as its ring-opening will ruin the cyclic (Baird-aromatic) delocalization, explained in a curve-crossing diagram depicting the energy changes of two triplet diradical structures localized to either the COT ring or the C_α-C_β bond of the cPr group (Figure 1A). In contrast, when attached to T_1 antiaromatic rings the cPr group should open particularly easily as its opening will alleviate antiaromaticity (Figure 1B). Yet, since the cPr group opens when next to a radical, and also a radical pair with triplet multiplicity, it will not differentiate between T_1 antiaromatic and nonaromatic rings. Instead, it should specifically identify T_1 state aromatic cycles. Moreover, as Baird's rule applies to the S_1 state we argue that the cPr group may also function for S_1 state aromaticity.

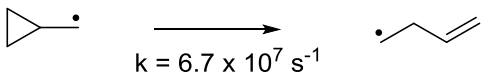

1

Scheme 1: Ring-opening of the cyclopropylcarbinyl radical (**1**).

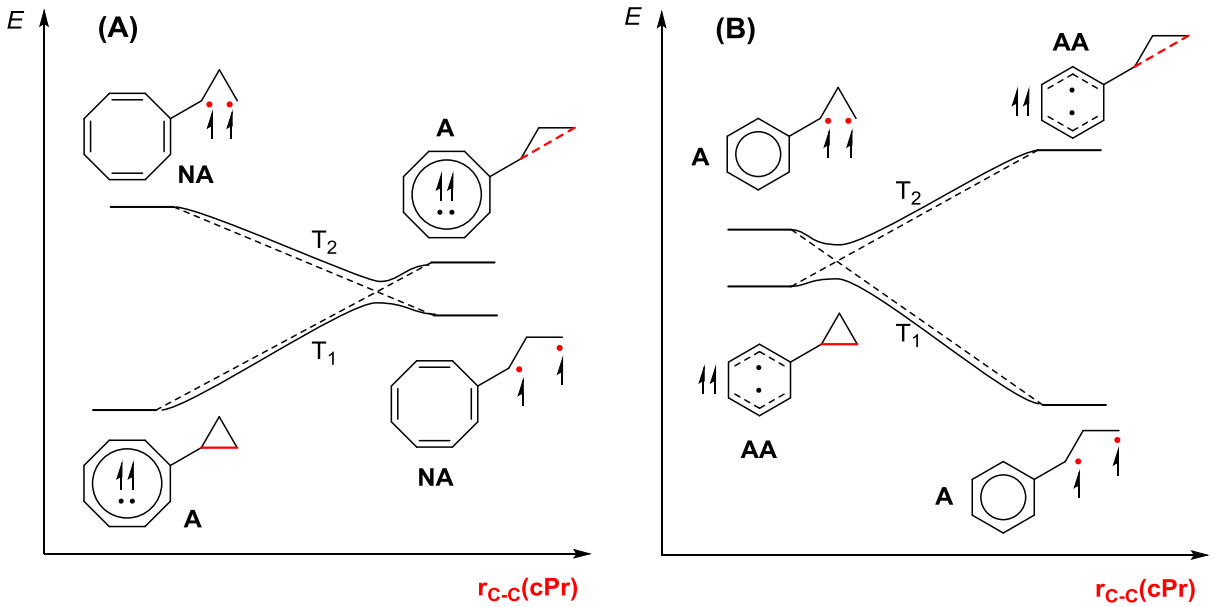

Figure 1: Curve-crossing diagram for the ring-opening of cyclopropylCOT (A) and cyclopropylbenzene (B) in their T_1 states in dependence of the C_α-C_β bond distance of the cPr group. The dissociating C_α-C_β bond and the corresponding two same-spin electrons of the cPr group are displayed in red. The (anti)aromaticity of the annulene is represented by A = aromatic, AA = antiaromatic, and NA = nonaromatic. Aromatic structures have low relative energies, nonaromatic intermediate and antiaromatic high energies. The aromatic structures are composites of several valence bond structures.

Three criteria should be fulfilled; (*i*) the cPr group must be a substituent on the potentially excited state aromatic cycle, (*ii*) the excitation must be localized to this cycle, and (*iii*) decay to the S_0 state must not be faster than ring-opening of the cPr group. The last requirement is complex since the persistence of the cPr group in a photochemical context depends on the activation barrier for its ring-opening *vs.* the rate for radiative and non-radiative decay processes as well as competing photochemical reactions.

We report on experimental studies of cPr substituted benzene, COT, naphthalene and biphenylene, whereby the excited state lifetimes of the parent compounds are important. The T_1 state lifetimes of these compounds are longer by factors 10^3 – 10^5 [33-36] (Table S1) than the lifetime of **1** (14.9 ns). Thus, the cPr ring-opening will not be restricted by T_1 state lifetimes. The situation is different in the S_1 state where the lifetimes of benzene and naphthalene are 28 – 34 ns and 96 - 105 ns, respectively.[34] The corresponding lifetime of COT is not reported, but for biphenylene it is merely 0.23 ns,[34] leading to the question if cPr ring-opening in the S_1 state of a cPr-substituted biphenylene will occur before it has decayed to the S_0 state.

One can argue that several different photoreactions (*e.g.*, carbon-halogen bond dissociation and olefin *Z*/*E*-photoisomerizations)[2,3] can be used to identify excited state

aromatic compounds. But as those structural units have either lone-pairs, leading to nπ* states, or additional π-orbitals that influence ground and/or excited states we find the cPr group to be more suitable as a potential excited state aromaticity indicator, although its scope and limitations must be resolved. In an applied context it can be noted that the cPr group is an often found unit in drug molecules.[37] Our present study indicates in which π-conjugated structural environments this group will be stable to light, information of potential use for drug design.

Results and Discussion

To determine if the cPr group can distinguish a T_1 state aromatic cycle from one which is T_1 antiaromatic or nonaromatic we first used quantum chemical computations to examine the T_1 state potential energy surfaces (PESs) for cPr ring-opening of compounds **1** – **15** as well as their spin density distributions. We further calculated the S_1 state PESs of cyclopropylbenzene (**10**) and cyclopropylCOT (**11**). We excluded cyclopropylCBD as CBD is reported to be only weakly T_1 aromatic.[38,39] Experimentally we studied the photostabilities of **10**, **11**, 2-cyclopropylnaphtalene (**13**), and 2-cyclopropylbiphenylene (**15**), both upon direct and sensitized irradiation in presence of methanol as trapping agent. Subsequently, we used quantum chemical computations to assess changes in (anti)aromaticity along the T_1 PESs of **8** – **15**, and we explored how the findings extend to the $^3\pi\pi^*$ states of the heterocyclic compounds **16** – **31**.

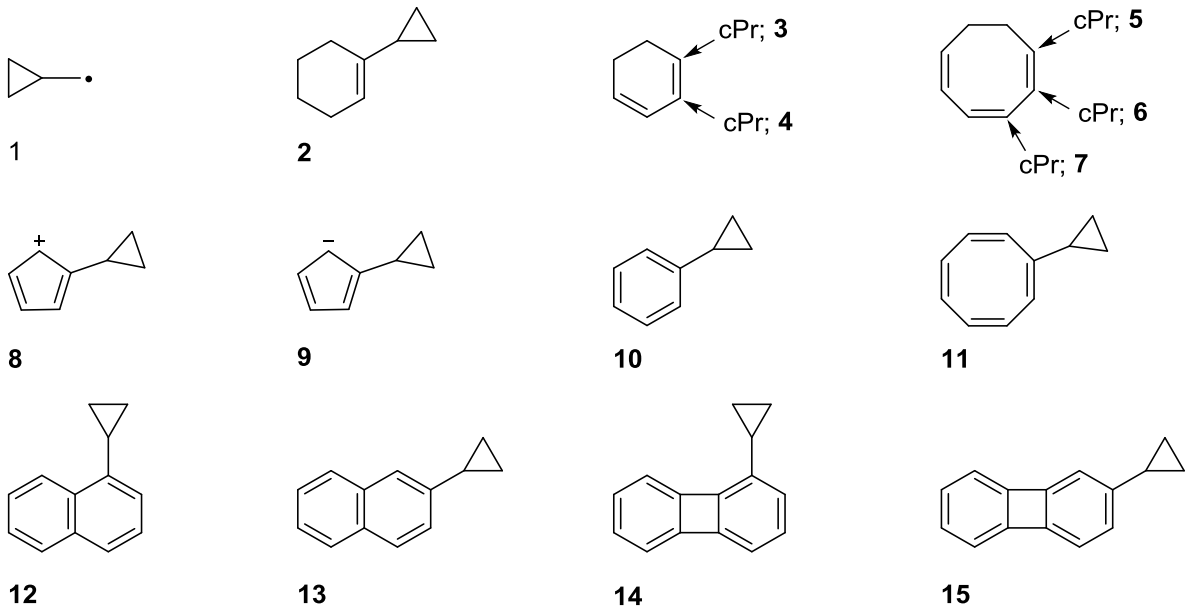

Figure 2: The all-carbon compounds investigated; the cyclopropylcarbinyl radical (**1**), 1-cyclopropylcyclohexene (**2**), cyclopropylcyclohexa-1,3-dienes (**3** and **4**), cyclopropylcyclo-octa-1,3,5-trienes (**5** - **7**), the cyclopentadienyl cation and anion (**8** and **9**), cyclopropylbenzene (**10**), cyclopropylCOT (**11**), 1-cyclopropylnaphthalene (**12**), 2-cyclopropylnaphthalene (**13**), 1-cyclopropylbiphenylene (**14**) and 2-cyclopropylbiphenylene (**15**).

Nonaromatic reference compounds: The cyclopropylcarbinyl radical (**1**) and compounds **2** – **7** are nonaromatic references against which **8** – **15** are evaluated. At UB3LYP/6-311G(d,p) level the activation free energy for ring-opening of **1** in its doublet ground state is 7.1 kcal/mol and the reaction energy is -5.0 kcal/mol (Figure 3), in agreement with previously computed and experimental values.[28-30] For **2** – **7** in their T_1 states the calculated activation energies are 6.1 – 21.1 kcal/mol, and the reactions are exergonic by 1.3 – 21.0 kcal/mol. Noteworthy, there is a good correlation (R^2 = 0.931, Figure 4) between the activation energies of **1** – **7** and the spin densities at the C atoms to which the cPr groups are

attached. For similar plots using Mulliken (R^2 = 0.941) and NPA (R^2 = 0.916) spin densities, see the Supporting Information.

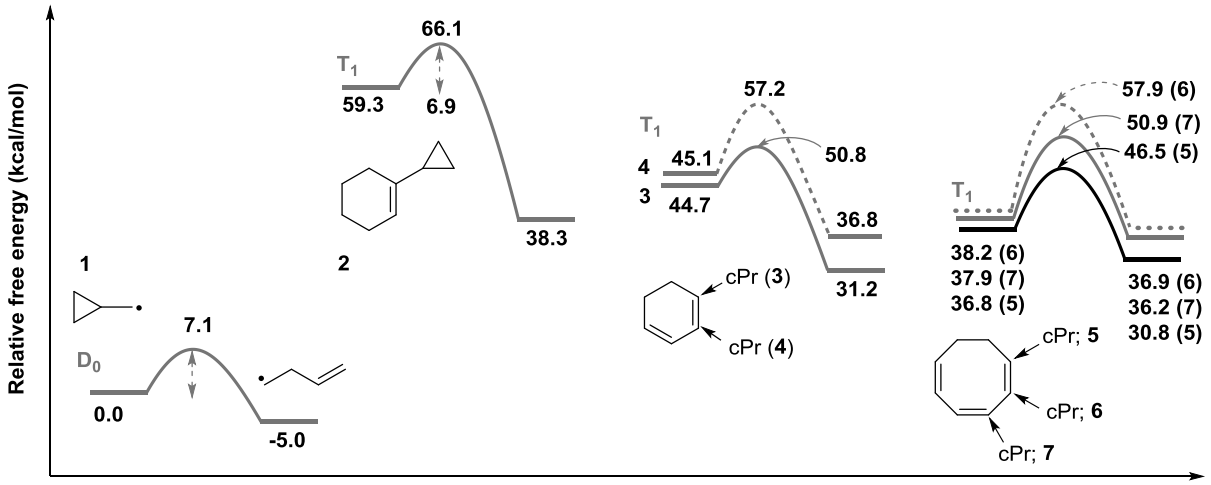

Figure 3: T_1 (D_0 for **1**) state potential energy surface diagrams for the cyclopropyl ring-openings of **1** - **7** at UB3LYP/6-311G(d,p) level.

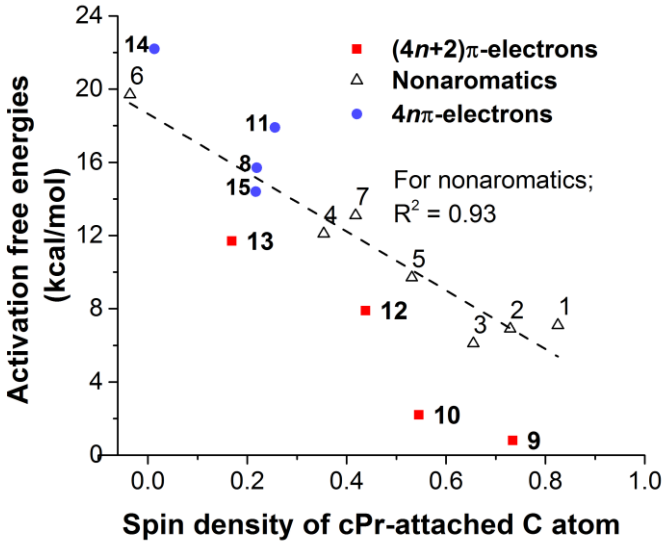

Figure 4: Activation free energies of cPr ring-opening in dependence of the spin density (QTAIM) at the C atom at which the cPr group is attached, with a least-squares fit of the data for the nonaromatic reference compounds **1** - **7**. Positive values represent excess of α-spin

10.1002/chem.201701404

density, negative values excess of β-spin density. Open triangles for nonaromatic, filled squares for compounds **9**, **10**, **12**, and **13**, and filled circles for **8**, **11**, **14**, and **15**.

cPr-Substituted annulenic compounds 8 – 11 in the T_1 state: Now, are the activation energies higher for the T_1 aromatic compounds than for the nonaromatic references, and is it the opposite for T_1 antiaromatic ones? Also, are the reaction energies more endergonic (exergonic) for the T_1 aromatic (antiaromatic) compounds than for the references? The activation energies for **8** and **11** with $4n\pi$-electron cycles are higher (16 – 18 kcal/mol, Figure 5) than all except one reference (**6**), while those of **9** and **10** are much smaller (1 – 2 kcal/mol). Moreover, the reaction energies are strongly endergonic for **8** and **11** while they are markedly exergonic for **9** and **10**.

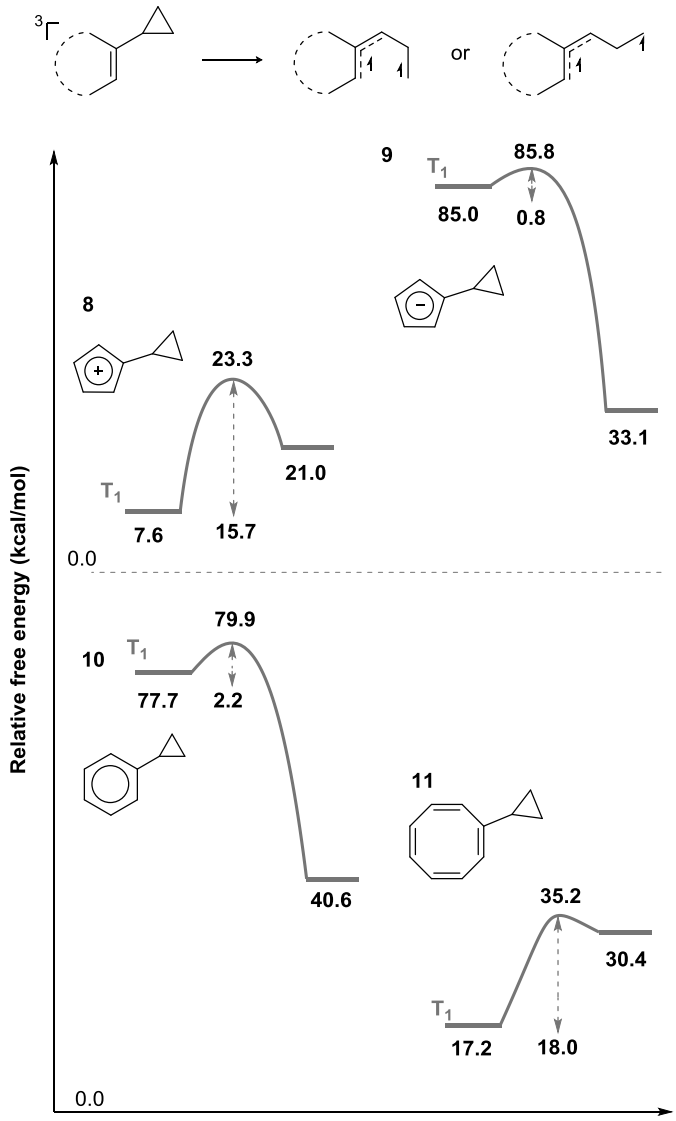

Figure 5: T_1 state potential energy surface diagrams for cyclopropyl ring-openings of **8** - **11** at the UB3LYP/6-311G(d,p) level.

Noteworthy, the T_1 state cPr ring-opening reactions of **8** – **11** are all adiabatic according to intrinsic reaction coordinate (IRC) calculations as the transition states are smoothly connected to both reactants and products (Figures S53-S56). The IRC plots closely resemble the T_1 PES diagrams of Figure 5. Moreover, the vertically excited T_2 state computed with TD-UB3LYP//UB3LYP along the T_1 state IRC paths of **10** and **11** reveal relationships between the T_1 and T_2 states (Figures S61- S62) that resemble the qualitative curve-crossing diagrams of Figure 1. At the TS structures of **10** and **11**, the T_2 states are calculated to be,

respectively, 26.7 kcal/mol (1.16 eV) and 42.4 kcal/mol (1.84 eV) above the T_1 states. The same picture results at CASPT2//B3LYP level where the energy differences are 1.51 and 1.70 eV, respectively (Figures S63- S64). With regard to the T_1 state minimum geometries of **10** and **11** the benzene ring in **10** is best described as antiquinoid as drawn in Figure 1B,[40] while the COT ring in **11** is nearly octagonal as depicted in Figure 1A with CC bonds length in range 1.398 – 1.414 Å.

Do the activation energies for cPr opening reflect the number of π-electrons in the annulenic cycles? In a T_1 aromatic cycle the two unpaired same-spin π-electrons will be delocalized leading to low spin density per C atom, and accordingly, a lowered propensity for cPr ring-opening. Additionally, we find that the activation barrier is linked to the number of π-electrons of the ring (4*n* or 4*n*+2) because for the two (4*n*+2)π-electron compounds **9** and **10** the activation energies are well below the regression line for the nonaromatic references (-6.1 and –7.7 kcal/mol, Figure 4 and Table S2). Oppositely, for the 4*n*π-electron compound **11** the activation energy is 3.4 kcal/mol above the line, while for **8** it is situated on. However, the activation energy of **8** it likely reduced because the two C_α-C_β bonds are significantly elongated (1.571 Å) at the T_1 state minimum. Indeed, when combined with results of cPr-substituted heterocycles (*vide infra*) our findings suggest that there is a drive to alleviate T_1 antiaromaticity of 4*n*+2 π-electron cycles and a resistance to give up T_1 aromaticity of 4*n* cycles.

cPr-Substituted polycyclic compounds 12 – 15 in the T_1 state: Naphthalene is antiaromatic in its T_1 state,[16] and we now find the cPr ring-openings of **12** and **13** to be exergonic (Figure 6) but less so than for **10**. Moreover, the activation energies are higher (8 – 12 kcal/mol) than that of **10** and resemble those of **1** - **7**. The activation energy of **13** is higher than for **12**, and our calculations show that the spin density at the C atom to which the cPr group is attached has an influence on the activation barrier because a higher spin density is

observed for C1 in **12** (0.558) than for C2 in **13** (0.167). Yet, for both **12** and **13** the activation energies are lower by ~4 kcal/mol when compared to the nonaromatic reference line, again revealing an additional driving force for cPr ring-opening when compared to that predicted exclusively from the spin density (Table S2).

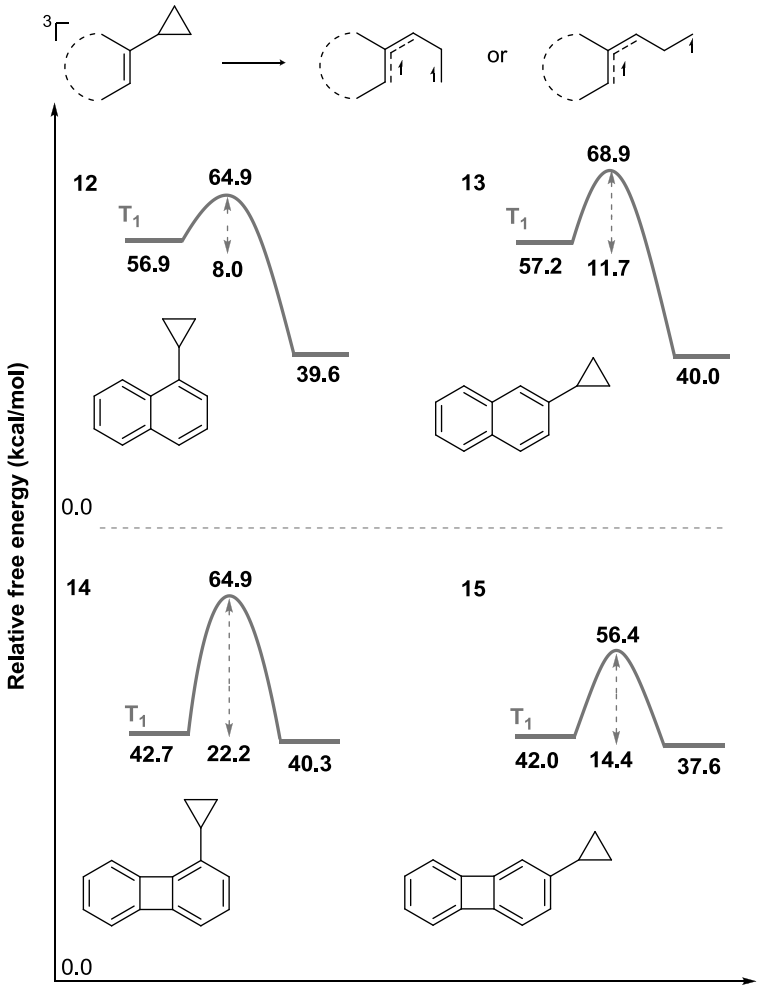

Figure 6: T_1 state potential energy surface diagrams for cyclopropyl ring-openings of **12** - **15** at UB3LYP/6-311G(d,p) level.

Biphenylene is an "aromatic chameleon" compound (Figure 7) as it can adapt to different aromaticity rules; Hückel's rule in the S_0 state and Baird's rule in the T_1 and S_1 states.[2,41-43] For the cPr substituted biphenylenes **14** and **15** the ring-opening reactions in the

T_1 states are modestly exergonic (Figure 6). Yet, the activation energy of **14** is even higher than that of **11**. The activation energy of **15**, on the other hand, is 14.4 kcal/mol, slightly lower than reported for the T_1 state *Z*/*E*-photoisomerization of 3-(prop-1-enyl)perylene (15.7 kcal/mol), a reaction that progressed slowly at ambient temperature.[44] When compared to the non-aromatic **2** – **7**, compounds **14** and **15** displayed less exergonic ring-opening reactions, and the activation energies are high. Thus, the T_1 PESs of **14** and **15** resemble those of the 4*n*π-electron species **8** and **11** more than those of the (4*n*+2)π-electron compounds **9** and **10**, suggesting 12π-electron circuits in the T_1 states of **14** and **15**. Indeed, for **14** the activation energy is 3.8 kcal/mol higher than expected had it been nonaromatic (Figure 4), but for **15** the activation energy is predicted as were it nonaromatic.

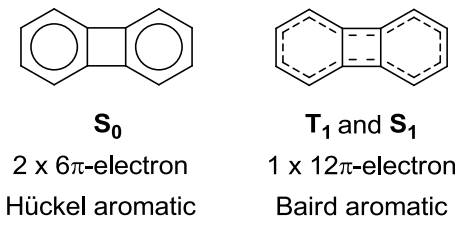

Figure 7: Aromatic resonance structures of biphenylene showing the "aromatic chameleon" characteristics of this compound in its S_0 *vs*. T_1 and S_1 states.

Computed S_1 state PESs of 10 and 11: We also computed the reaction and activation free energies of **10** and **11** in the S_1 states at CASPT2/ANO-RCC-VTZP//CASSCF/6-31G(d) level using, respectively, (8in8) and (10in10) active spaces. The benzene ring in the calculated S_1 state structure of **10** resembles that earlier found for benzene,[45] and the relaxation of **10** from the Franck-Condon region should resemble that of benzene.[46] Moreover, it has earlier been concluded that the D_{8h} symmetric COT is a collecting point on the S_1 state surface,[47] and also **11** in the S_1 state has a nearly octagonal COT ring.

The reaction free energies for ring-opening of the cPr group are 12.7 kcal/mol for **10** and 54.3 kcal/mol for **11** at MS-CASPT2/ANO-RCC-VTZP level (Figure 8). The CASPT2 calculations reveal that the S_1 and S_2 states of **10** become degenerate, but only after the transition state structure (Figure S63). Moreover, the activation free energy for cPr ring-opening of **10** in the S_1 state is 13.4 kcal/mol, *i.e.*, 11.2 kcal/mol higher than in the T_1 state at (U)B3LYP/6-311G(d,p) level. For **11**, the transition state for the ring-opening was not possible to locate, likely due to a degeneracy between the S_2 and S_3 states close to the transition state regions (see Figures S67-S69). Instead, using a linear interpolation approach we estimate the activation energy at 68.0 kcal/mol, much higher than for the T_1 state. Yet, despite the fact that both ring-opening reactions are endergonic, the much higher endergonic reaction energy of **11** than of **10** shows a trend that lends support to our hypothesis also in the S_1 state; loss of S_1 state aromaticity seems to be a particularly unfavorable process. For mappings of the higher excited states of **10** and **11** see the Supporting Information.

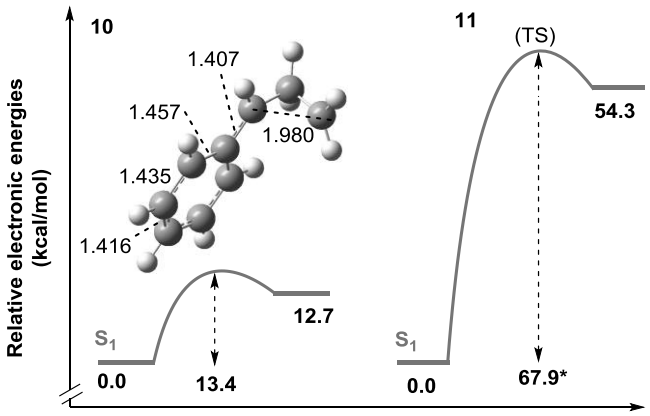

Figure 8: The S_1 state PESs of **10** and **11** at the CASPT2/ANO-RCC-VTZP//CASSCF/6-31G(d) level, with the reference energies being the energies of the ring-closed species in their S_1 states. For **11**, a linear interpolation method is used for finding the transition state. Active spaces and occupation numbers are described in the Supporting Information (Tables S3-S7).

Experimental studies of 10, 11, 13 and 15: Compounds **11**, **13** and **15** were prepared by a slight modification of a procedure by Paquette and co-workers (for synthetic details see the SI).[18] However, the yields of cyclopropanation decreased gradually when going from COT to benzene (Scheme 2), and only starting material was recovered when bromobenzene was used. Yet, **10** is commercially available.

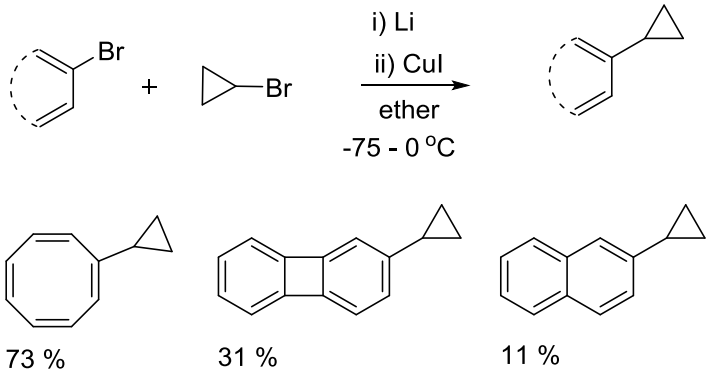

Scheme 2: Synthesis of cyclopropyl substituted compounds.

Compound **10** has its first UV absorption at 274 nm, and upon irradiation of a 14.5 mM solution of **10** in methanol with $\lambda = 254$ nm for two hours it formed the ring-opened methoxy adduct **10-MeOH$_{ad}$** (Scheme 3). Continuous monitoring of the reaction with GC-MS showed that **10** has photodecomposed completely after twelve hours (Figure 9A). The formation of **10-MeOH$_{ad}$** reached a photostationary state after ten hours, but the conversion to **10-MeOH$_{ad}$** is merely 3% according to GC-MS. Long-term irradiation (24 h) gave only polymers according to spectral analysis (see Figures S13-S18). This polymer formation progresses via **10-MeOH$_{ad}$** as supported by irradiation of separately prepared **10-MeOH$_{ad}$** leading to yellowish polymers (see Figures S23-S28 for NMR and UV-Vis spectra, and photos of reaction tubes). Since benzene has an intersystem crossing quantum yield (Φ_{ISC}) of 0.25,[48] the photodegradation of **10** likely arises from its T_1 state, or from both the S_1 and T_1 states as a substantial difference in yields of the photodecomposition products was observed when a solution of **10** was irradiated with and without oxygen present (Figure 9B).

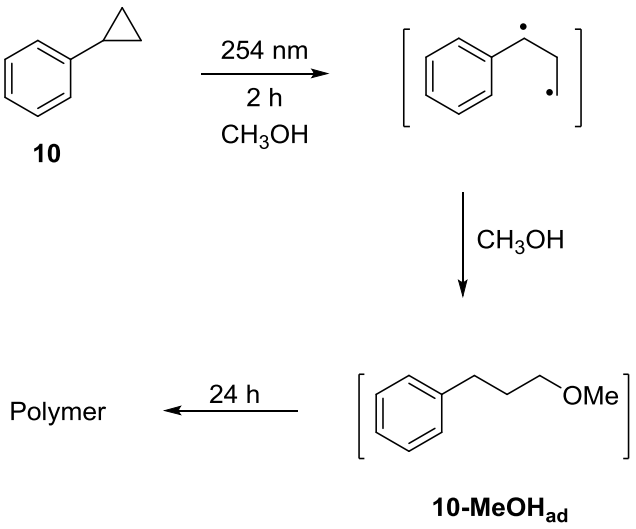

Scheme 3: Photoreaction of **10** with MeOH.

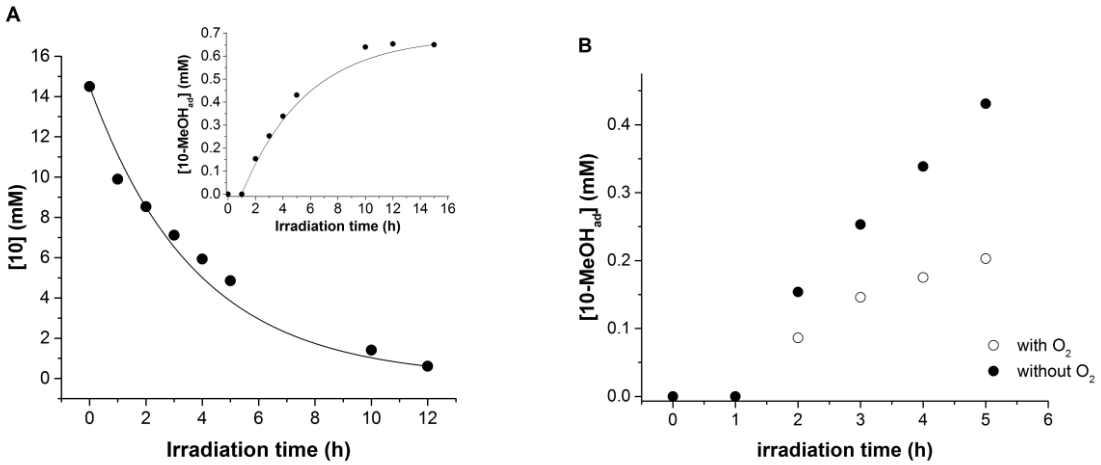

Figure 9: (A) Concentration of **10** as a function of irradiation time with inset showing the formation of the adduct (**10-MeOH$_{ad}$**) formed between **10** and methanol, and (B) a comparison of the increase in concentration of **10-MeOH$_{ad}$** when oxygen is present and when not.

Direct irradiation of an 11 mM solution of **13** in methanol at λ = 254 nm for 24 hours, and continuous monitoring with GC-MS, revealed that its decomposition is slower than

that of **10** (see Figures S36 – S40). As naphthalene has an Φ_{ISC} of 0.75 [49] the process likely progresses in the T_1 state. The ring-opened adduct (**13-MeOH$_{ad}$**) appears after seven hours and reaches a maximum after eleven hours (to a conversion of merely <1%). Compound **13**, which should be labeled as T_1 antiaromatic based on both previous findings for naphthalene[16] and our computations (*vide infra*) has decomposed fully after 24 hours. Here it should be noted that the molar absorptivity of naphthalene (~3500 $M^{-1}cm^{-1}$) is more than an order of magnitude higher than that of benzene (~215 $M^{-1}cm^{-1}$), yet, the rate of cPr ring-opening is considerably slower in **13** than in **10** (Figure S41). Thus, the difference in the observed rate of cPr ring-opening is not related to the difference in absorptivity but most likely due to the higher activation barrier for cPr opening in **13**.

Our hypothesis as well as computations predict a drastically different reactivity of **11** when compared to **10** and **13**. Indeed, when **11** was irradiated for 24 hours in presence of methanol at 254 nm only starting material was recovered (Scheme 4). As COT has a very low Φ_{ISC} [35] this finding applies to the S_1 state, and it is in line with the high calculated S_1 state activation barrier of **11** (Figure 8) or short S_1 lifetime. Yet, **11** can be excited to the T_1 state since efficient energy transfer from triplet pyrene and anthracene to COT takes place.[35] Still, **11** is recovered unreacted when irradiated at 300 nm in presence of triplet sensitizers, and we conclude that the cPr ring is not opened because an intermediate would have been trapped by MeOH. This low reactivity is in line with the observation by Paquette and co-workers that dialkyl-COTs in presence of acetone are persistent to photolysis.[16,18] Our data show that even an alkyl substituent which normally is labile to (di)radical character remains unaffected when COT is irradiated. This is a strong indication that the cyclopropyl group can identify excited state aromatic cycles. Yet, what is the situation for more complex polycyclic molecules influenced by excited state aromaticity, *e.g.*, biphenylene?

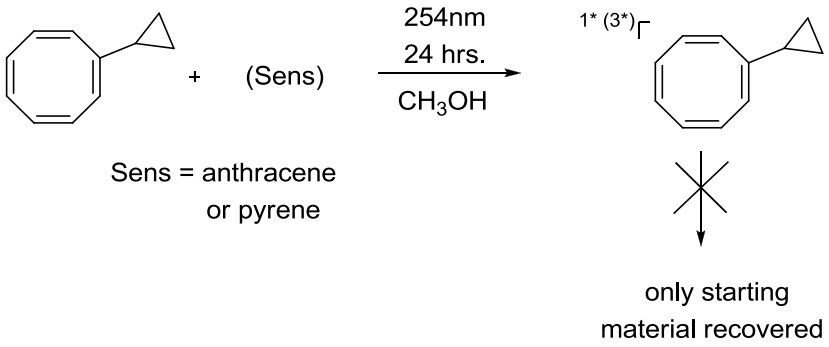

Scheme 4: Photoreactions of **11** with MeOH, with or without sensitizer.

Indeed, there is literature support for photochemical persistence of cyclopropylbiphenylene derivatives because Wu and co-workers synthesized such species by a photochemical route (λ = 254 nm).[50] The UV absorption spectrum of **15** shows a major absorption at λ = 255 nm and a small band at around 300-350 nm (see Figure S50), resembling the published spectrum of biphenylene.[51] Interestingly, no ring-opening was observed upon direct irradiation of a 16 mM solution at λ = 254 in presence of methanol, not even after 24 hours of irradiation. However, this lack of photoreactivity can be connected to the short S_1 state lifetime (0.23 ns) [25] when compared to the lifetime of cyclopropylcarbinyl radical (14.9 ns). [52-54,36] Moreover, as the activation energy for cPr ring-opening in the S_1 state likely is equally high or higher than in the T_1 state, and as the Φ_{ISC} of biphenylene is low ($\Phi_{ISC} \leq 0.01$),[52] it is presumable that photoexcited **15** decays to the S_0 state before the cPr group can open. This reveals a limitation of the cPr group as an excited state aromaticity indicator.

When naphthalene was used as a triplet sensitizer in fivefold excess **15** was fully decomposed after 14 h, however, also the concentration of naphthalene decreased continuously in this process (Figures S43 – S45). In contrast, only starting material is recovered if we irradiate a 5 mM solution of **15** in MeOH at 254 nm for 24 hours in presence of Xe, known to increase the spin-orbit coupling and intersystem-crossing due to the heavy

atom effect.[55] According to our calculations the cPr group of **15** opens over a barrier of 14.4 kcal/mol, possible to overcome in the T_1 state but only slowly, resembling the *Z*/*E*-photoisomerization of 3-(prop-1-enyl)perylene.[44] This combined suggests that **15** is photostable when the reaction is performed under constant supply of Xe.

Changes in excited state (anti)aromaticity upon cPr ring-opening: To what extent are the shapes of the T_1 state PESs for cPr ring-openings of **8** – **15** connected to changes in (anti)aromaticity? We first compared the potentially T_1 aromatic **8** and **11** against the potentially T_1 antiaromatic **9** and **10** using HOMA (harmonic oscillator model of aromaticity) and ACID (anisotropy of the induced current density) plots, and subsequently analyzed the polycyclic **12** – **15**. Changes in S_1 state (anti)aromaticity in **10** and **11** were only assessed via changes in CC bond lengths.

The HOMA values of ^{3}**8-closed** and ^{3}**11-closed** are both positive, and for ^{3}**11-closed** it corresponds to a strongly aromatic COT cycle (Figure 10). Similarly, the ACID plots show that both compounds have diatropic (aromatic) ring-currents. Cyclopropyl ring-opening, giving ^{3}**8-open** and ^{3}**11-open**, leads to structures with lowered HOMA values and loss of the diatropic ring-currents according to the ACID plots. This reveals loss of T_1 aromaticity. In contrast, for ^{3}**9-closed** and ^{3}**10-closed**, which have 6π-electron cycles, the HOMA values are negative indicating antiaromatic character (Figure 10), and this is supported by paratropic (antiaromatic) ring-currents. Upon cPr ring-opening, leading to ^{3}**9-open** and ^{3}**10-open**, respectively, the compounds go from antiaromatic to aromatic; in particular the HOMA of ^{3}**10** increases by 1.308 to 0.861. Taken together, ^{3}**8** and ^{3}**11** *versus* ^{3}**9** and ^{3}**10** display opposite changes in their (anti)aromatic characters upon cPr ring-opening. This connects well with the shapes of the T_1 PESs; in **8** and **11** T_1 aromaticity is lost in the endergonic cPr ring-openings while **9** and **10** alleviate T_1 antiaromaticity in strongly exergonic processes.

10.1002/chem.201701404

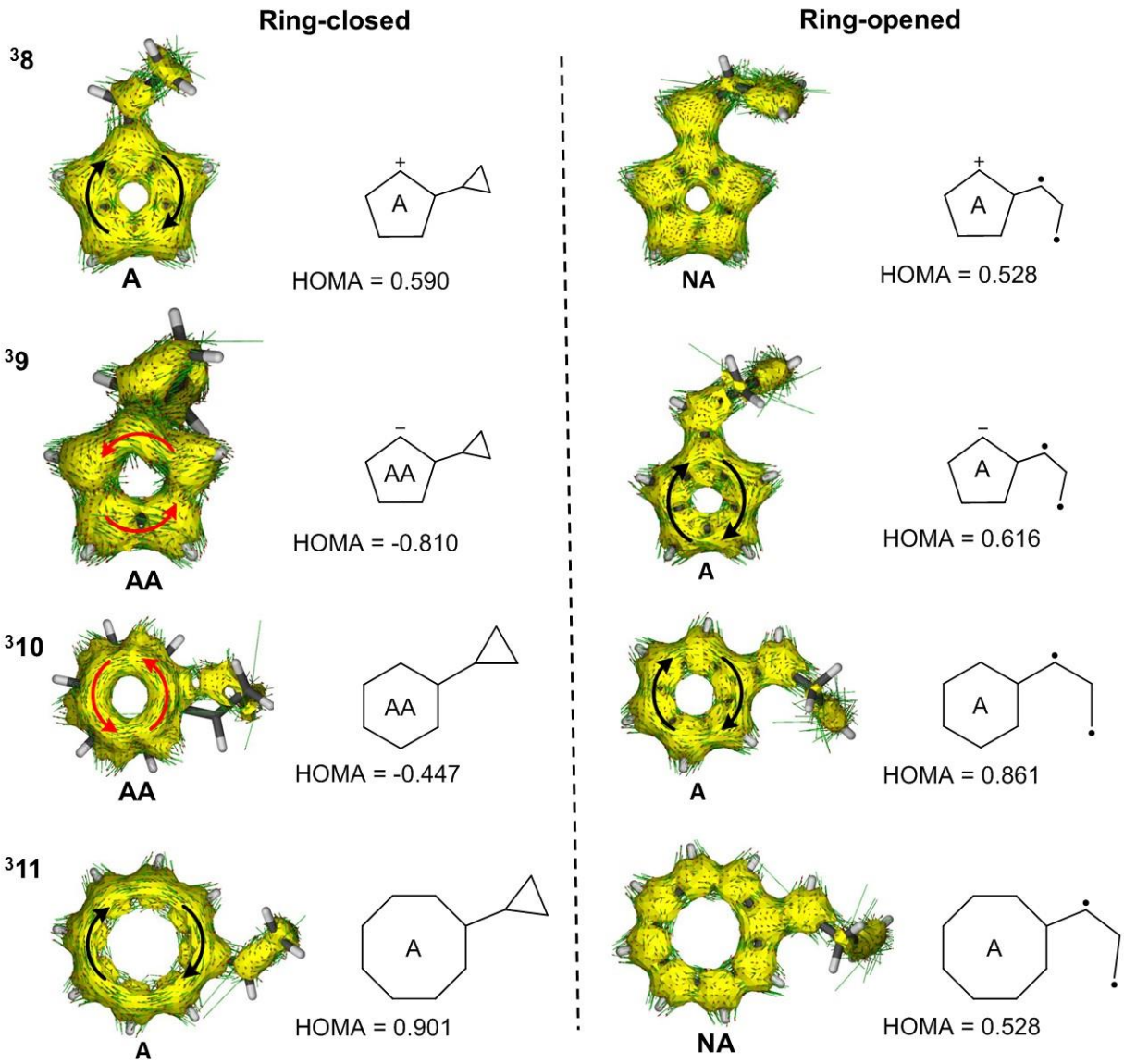

Figure 10: ACID plots of **^{3}8** – **^{3}11** at (U)B3LYP/6-311+G(d,p)//(U)B3LYP/6-311G(d,p) level (for larger images see the Supporting Information) and HOMA values at the (U)B3LYP/6-311G(d,p) level. Black clockwise arrows represent diatropic (aromatic) ring-currents and red counter-clockwise arrows paratropic (antiaromatic) ring-currents. A = aromatic, NA = non-aromatic and AA = antiaromatic.

For cPr-substituted naphthalenes **^{3}12-closed** and **^{3}13-closed**, the HOMA(peri) values, *i.e.*, the HOMA values based on the CC bonds of the perimeter, suggest weakly aromatic character while the ACID plots show paratropic ring-currents (Figure 11). Yet, both

10.1002/chem.201701404

HOMA and ACID reveal that cPr ring-opening, leading to ^{3}**12-open** and ^{3}**13-open**, is linked to antiaromaticity relief and aromaticity gains in line with the exergonic reaction energies of Figure 6.

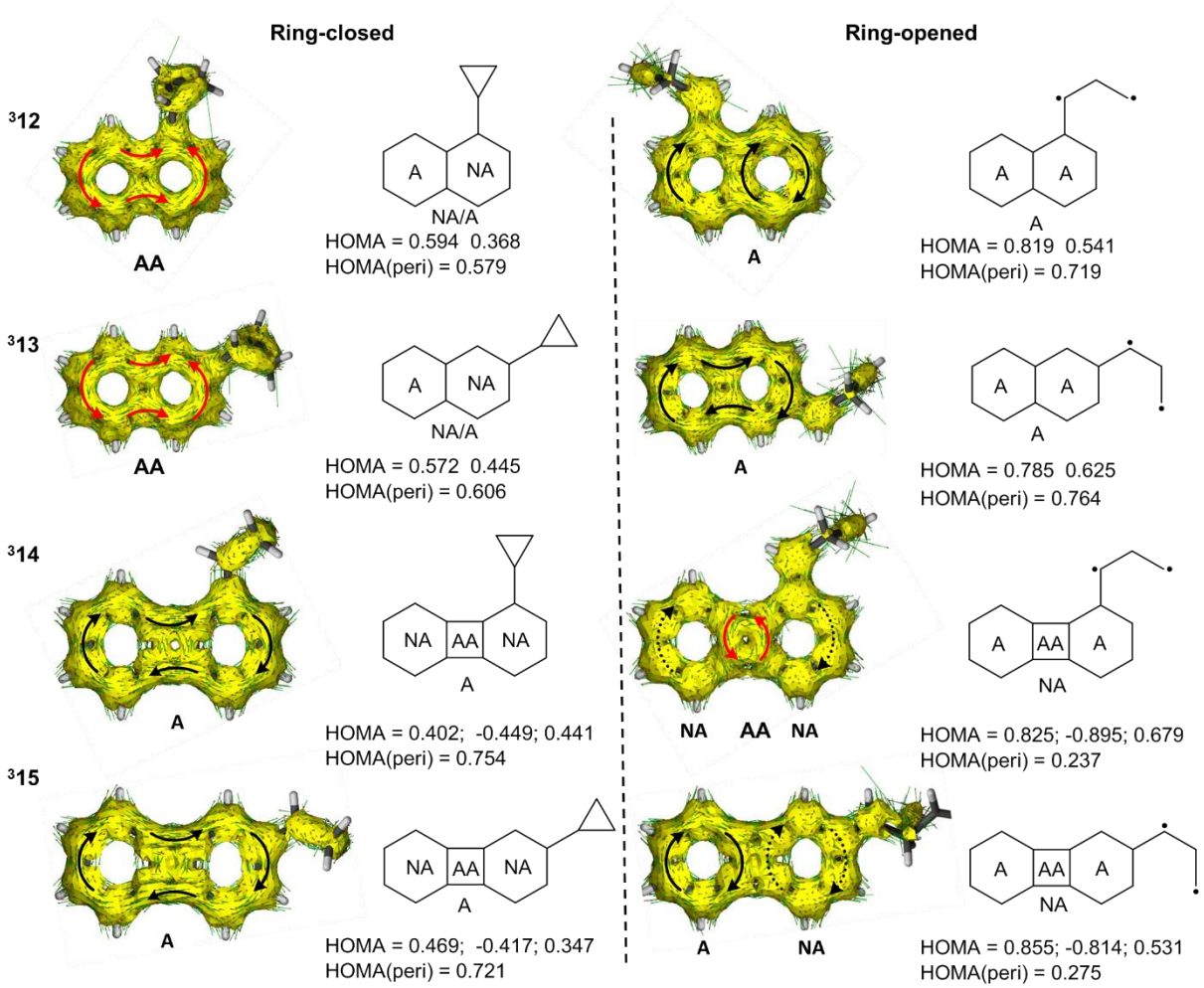

Figure 11: ACID plots of ^{3}**12** – ^{3}**15** at (U)B3LYP/6-311+G(d,p)//(U)B3LYP/6-311G(d,p) level (for large images see the Supporting Information) and HOMA values at (U)B3LYP/6-311G(d,p) level. Black clockwise arrows in the ACID plots represent diatropic (aromatic) ring-currents and red counter-clockwise arrows represent paratropic (antiaromatic) ring-currents. The HOMA values for the perimeters are indicated as HOMA(peri). A = aromatic, NA = non-aromatic and AA = antiaromatic.

The perimeters of ^{3}**14-closed** and ^{3}**15-closed** are influenced by Baird-aromaticity according to both HOMA (HOMA(peri) = 0.754 and 0.721, respectively) and ACID plots displaying diatropic ring-currents, in line with biphenylene being an aromatic chameleon (Figure 7). This T_1 aromaticity is disrupted upon ring-opening, but as the compounds are polycyclic the (anti)aromatic features of the ring-opened isomers are complex. Moreover, and opposite to **8** and **11**, the process is neither particularly exergonic nor endergonic since ^{3}**14-open** and ^{3}**15-open** can adopt some local (Hückel-)aromatic character in the six-membered rings. Clearly, polycyclic molecules pose limitations to the usage of the cPr group as an excited state aromaticity indicator.

Finally, in the S_1 state we only consider **10** and **11**. In **10-closed** all CC bond lengths in the benzene ring are nearly equal (1.431 - 1.441 Å) while upon ring-opening they become alternating single and double bonds (1.364 – 1.461 Å, see Figure S70 for plots of bond length alternation). The significant CC bond elongation in **10-closed** is noteworthy and could be a collective response which alleviates a strongly antiaromatic character at the vertically excited S_1 state structure. In the S_1 state of **11-closed** the CC bonds in the COT ring are found within 1.404 – 1.417 Å, and the bond length alternation in **11-open** (1.395 – 1.423 Å) is also small when compared to that in **10-open** (see Figure S71).

cPr-Substituted heterocycles with 4n or 4n+2 π-electrons: Many heterocyclic compounds are aromatic in their S_0 states,[56] and can be T_1 and S_1 state antiaromatic provided these states are of ππ* instead of nπ* character. However, as heteroatoms have different electronegativities than carbon, excited state antiaromaticity can be attenuated through electron density redistributions. Moreover, electronegativity differences and/or poor size matches between the p_π-AOs of heteroatoms and those of carbons can weaken the π-conjugation and aromaticity.[57] Accordingly, both (4*n*+2)π- and 4*n*π-electron heterocycles may display properties that resemble those of the T_1 nonaromatic **2** – **7**. We examined a

selection of heterocyclic compounds with cPr substituents at the various positions and with ππ* T_1 states. We excluded 2- and 3-cyclopropylpyridine and 2-cyclopropylthiophene as their T_1 states are of nπ* character. Moreover, we did not consider S_1 state processes as this part of the study explores to what extent the nature of the heterocycles ($4n\pi$ *vs.* $(4n+2)\pi$) influences the activation and reaction energies. Are there similar effects in the T_1 states of cPr substituted heterocycles as in compounds **8** - **11**?

The cPr substituted 6π-electron heterocycles **26** - **31** showed highly exergonic cPr ring-opening reactions (Figure 12), but less so than **10**, indicating weakened T_1 antiaromaticity. Among the cPr substituted heterocycles with $4n$ π-electrons (**16** – **25**) nearly all had endergonic reaction energies. However, **16** and **18** have exergonic ring-opening reactions, likely due to poor heteroatom-carbon π-overlap yielding T_1 nonaromatic compounds. Among the cPr-substituted azepins (**19** - **21**) and oxepins (**23** - **25**), the oxepins have 2 - 5 kcal/mol less endergonic reactions. Interestingly, the N-cyclopropyl substituted $4n\pi$-electron compounds **17** and **22** have considerably higher reaction energies than their carbon substituted isomers.

With regard to the activation energies it can first be noted that the N-cyclopropylated compounds have significantly higher activation barriers than those with the cPr group attached at a C atom. Here, we focus on the latter isomers. The activation energies of all compounds with 6π-electron cycles, except **28**, have similar or slightly higher barriers to cPr ring opening than **10**. Importantly, all 6π-electron compounds with cPr substituents attached to a C atom have activation energies which are lower by 4 - 5 kcal/mol than the nonaromatic reference line (Figure 14 and Table S2). The situation is different for the 8π-electron azepins **19** – **21** as they have activation barriers in the range 16 - 22 kcal/mol, and those of oxepins **23** - **25** are 14 – 22 kcal/mol. On the other hand, the 8π-electron compounds

16 and **18** have activation barriers similar to those of the nonaromatic **1** – **7**, revealing that when T_1 aromaticity is attenuated, the cPr group will open.

Now, combining the activation energies of the heterocyclic compounds **16** – **31** with those of the all-carbon species **8** – **15** it becomes clear that species with (4*n*+2)π-electron cycles generally have lower activation barriers than had they been nonaromatic (Figure 14). Conversely, the 4*n*π-electron species have higher barriers than estimated from the nonaromatic references.

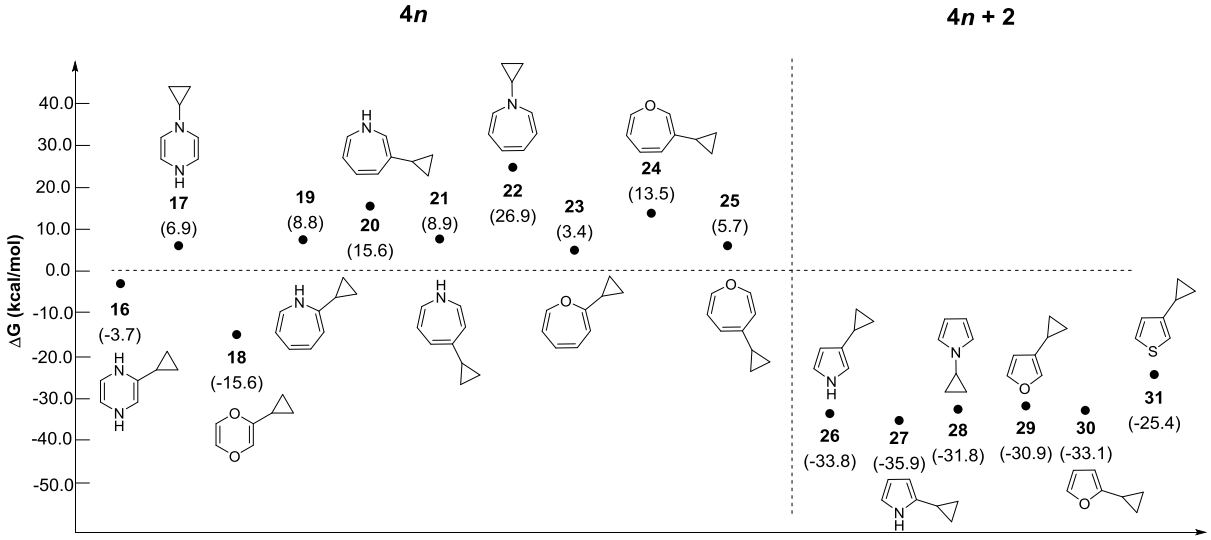

Figure 12: T_1 state Gibbs free energies of reaction of cyclopropyl ring opening of cyclopropyl substituted heterocycles with either 4*n* or 4*n*+2 π-electrons.

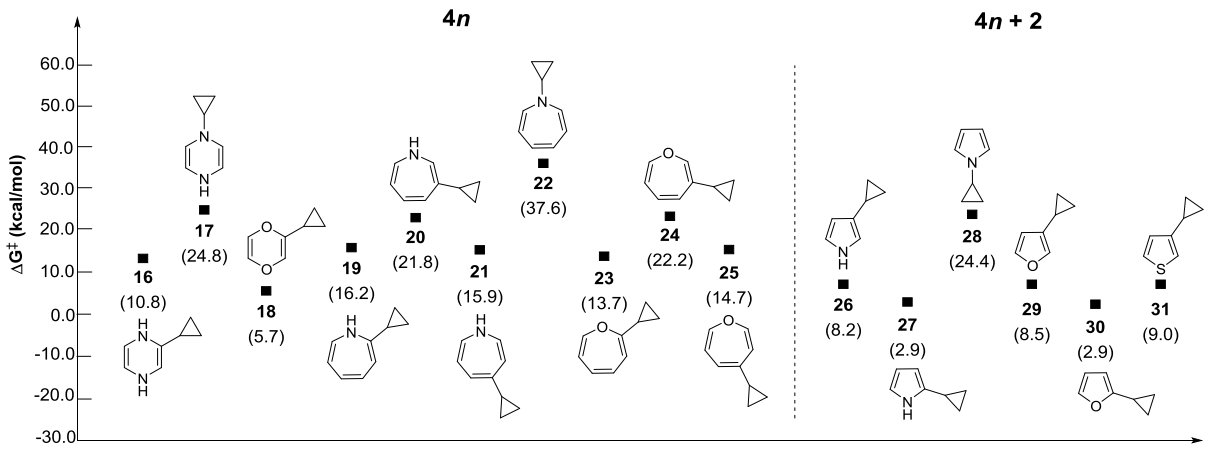

Figure 13: Activation free energies at the (U)B3LYP/6-311G(d,p) level for cyclopropyl substituted heterocycles with 4*n* and 4*n* +2 π-electrons in the T_1 state.

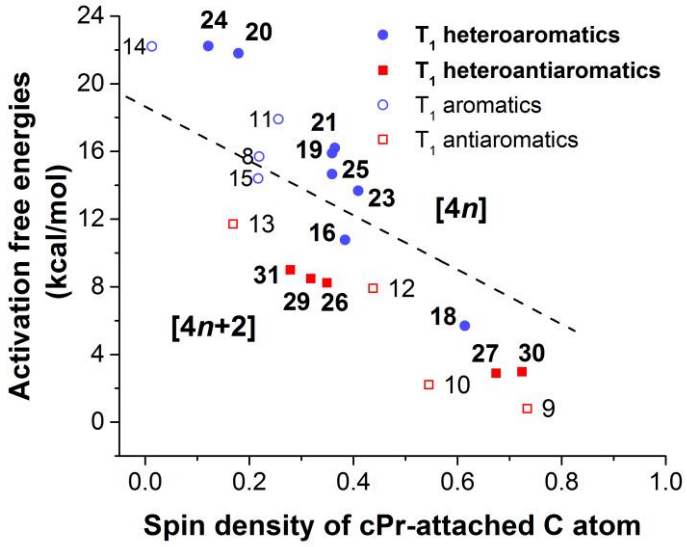

Figure 14: Activation free energies of cPr ring-opening of heterocycles **16** – **31** and all-carbon compounds **8** – **15** plotted against the spin density (QTAIM) at the C atom at which the cPr group is attached. The dashed line displayed is the regression in the least-squares fit of the data for nonaromatic reference compounds **1** – **7**. Positive spin density values represent excess of α-spin density, negative values excess of β-spin density. Filled circles for **16** – **25** and squares for **26** - **31**. Empty circles and squares for all-carbon T_1 aromatic and T_1 antiaromatic compounds, respectively.

Conclusions and Outlook

When a cyclopropyl substituted annulene is irradiated the effect on the cyclopropyl group is strongly determined by the excited state character of the annulene. The cPr group is known to act as a radical probe due to its tendency to ring-open when next to radicals and diradicals.[23,24] Yet, our hypothesis is that it remains closed when attached to an annulene which is T_1 and S_1 state aromatic as its ring-opening will ruin the ESA character. Indeed,

through comparison with nonaromatic compounds we reveal that cPr substituted 4*n*π-electron annulenes and heterocycles have T_1 state activation barriers for C_α-C_β cleavage of the cPr group where 1.6 – 6.0 kcal/mol result from resistance to loose T_1 aromaticity (Figure 14). In contrast, compounds with (4*n*+2)π-electron cycles have activation barriers that are lower by 1.7 – 7.7 kcal/mol than had they been nonaromatic. This reveals a drive to alleviate T_1 antiaromaticity.

Our computations show that 4*n*π-electron heterocyclic compounds with one heteroatom (*e.g.*, azepins and oxepins) will keep the cPr group closed. With several heteroatoms in the ring the T_1 aromatic character is weakened due to attenuated π-orbital overlap, and as a result, the latter species have calculated T_1 PESs resembling those of T_1 nonaromatic molecules. Polycyclic compounds influenced by excited state aromaticity are also complex since parts of the polycyclic moieties can adopt (Hückel-)aromaticity in the cPr ring-opened isomers, leading to greater stabilizations than what is the case for the corresponding isomers of those with monocyclic 4*n*π-electron units.

At this point it should be stressed that the cPr group differentiates excited state aromatic cycles from excited state antiaromatic and nonaromatic ones. A separate probe needs to be identified for the excited state antiaromatic cycles, one where antiaromaticity lowers the activation energy to such an extent that it exclusively ring-opens for excited state antiaromatic cycles. We postulate that cyclopentyl or cyclohexyl groups have this ability, yet, such studies will be reported separately.

Finally, from an applications perspective our study outlines in which π-conjugated structural environments the cPr group leads to light-sensitive *vs.* light-insensitive compounds, findings of potential use in pharmaceutical chemistry as the cPr group is frequently found in drug molecules.[37]

Materials and Methods

All chemicals required for the synthesis were purchased from Sigma Aldrich (> 97% purity) and used without further purifications. Compounds **11**, **13** and **15** were synthesized while **10** was purchased from Sigma Aldrich (> 99.0%). All solvents (*n*-heptane and methanol) used for photosolvolysis were anhydrous. Distilled pentane was used for coloumn chromatography and recrystallization. De-ionized water was used during synthesis. NMR spectra were recorded on Agilent MR (^{1}H-NMR at 399.97 MHz, ^{13}C-NMR at 100.58 MHz). ^{1}H-NMR and ^{13}C-NMR spectra were referenced against $CDCl_3$ at 7.26 ppm and 77.16 ppm, respectively.[58] Photoreactions were monitored with the Gas Chromatography – Mass Spectrometry (GC-MS). Split-injection (2μL injection volume; Split Ratio: 100:1; 250 ^{o}C inlet temperature; Flow Rate: 120 mL/min) was used for injecting samples. The starting temperature of the column oven was 70 ^{o}C (0.5 min equilibration time) and the ending temperature was 320 ^{o}C. The temperature rate was set to 20 ^{o}C/min resulting in a 12.5 min total run time. Helium was used as a carrier gas (flow rate: 1.2 mL/min). The column used was an Aligent 19091S-433: 325 ^{o}C: 30 m x 250 μm x 0.25 μm (front SS-inlet: He; out: vacuum). Masspectrometer: Source temperature: 250 ^{o}C, Quad-temperature 150 ^{o}C. Varian Cary 50 UV-visible spectrometer was used for recording the UV-Visible spectra in between 200 – 800 nm wavelength range. Elemental analysis of compound **15** was recorded at Eurofins Mikro kemi AB, Uppsala.

An RPR-100 Rayonet Photochemical Chamber Reactor was used for photostability and photosolvolysis study. Two different sets of lamps were used depending on the excitation wavelength of the experiment: a set of 16 UV lamps at 2537 Å with a total power of 35 W or a set of 16 UV lamps at 3000 Å with total power of 35 W. Photoreactions were performed on two different scales; 15 mL quartz cylindrical tubes (RQV-5: Rayonet; Ø 13 mm) were used for the medium-scale photoreactions and for the large-scale photoreactions cylinders made of quartz with 185 mL capacity (RQV-118: Rayonet; Ø 20 mm) were used.

Computational details

Most of the quantum chemical calculations were performed at the (U)B3LYP hybrid density functional theory with the Pople basis sets 6-31G(d)[59-61] and 6-311G(d,p)[62] using Gaussian 09 revision D.01.[63] Frequency calculations were carried out at the same level of theory to confirm stationary points with no imaginary frequencies. All transition states were confirmed by intrinsic reaction coordinate (IRC) calculations.[64] The Harmonic oscillator model of aromaticity (HOMA) was used as a structural index of aromaticity and values were calculated at the (U)B3LYP/6-311G(d,p) level.[65] For polycyclic molecules, HOMA(peri) values based on the CC bonds of the perimeter of whole molecules are also considered. Positives values close to one correspond to aromatic compounds, negative to antiaromatic compounds, and values closed to zero correspond to nonaromatic compounds. The Anisotropy of the Induced Current Density (ACID) was used for visualizing electron delocalization and ring currents.[66] ACID plots were generated with the ACID 2.0.0 program[67] using the Continuous Set of Gauge Transformations (CGST) method at the B3LYP/6-311+G(d,p) level.[68] The MOLCAS 8.1 quantum chemistry program package[69] was used to run CASSCF[70] and CASPT2[71] calculations with the ANO-RCC-VTZP[72] basis set. Compounds **10** and **11** were optimized in the S_1 state with CASSCF/6-31G(d) using state-average calculations of the two and three lowest singlet excited states using an active space of (8,8) and (10,10), respectively. The transition state (TS) of **10** was also confirmed by IRC analysis. For **11**, the TS was found by linear interpolation in internal coordinate method between the **^{1}11-closed** and **^{1}11-opened** optimized structures. The electronic energies were calculated by MS-CASPT2/ANO-RCC-

VTZP at the CASSCF/6-31G(d) optimized geometries. Frequency calculations were performed at CASSCF/6-31G(d) level to confirm the true minima and the transition states. Atomic spin densities were calculated according to the Mulliken,[73] Natural Population Analysis (NPA)[74] and the Quantum Theory of Atoms in Molecules (QTAIM)[75] schemes, with Gaussian09, NBO6[76] and Multiwfn 3.3.8 (using a grid spacing of 0.10 Bohr),[77] respectively.

Acknowledgements: We are grateful to the Erasmus Mundus EXPERTS III program for PhD scholarship to R.A., the Wenner-Gren Foundations, and the Swedish Research Council (grant 2015-04538) for financial support. Moreover, H.O. thanks Joakim Bergman and Per-Ola Norrby, AstraZeneca Gothenburg, for stimulating discussions on the cyclopropyl group in pharmaceutical chemistry. We also thank the SNIC (Swedish National Infrastructure for computing) through NSC (National Supercomputer Center), Linköping, and UPPMAX, Sweden for generous allotment of computer time.

References

[1] V. I. Minkin, M. N. Glukhovtsev and B. Y. Simkin, Aromaticity and Antiaromaticity: Electronic and Structural Aspects; John Wiley and Sons: New York, **1994**.

[2] M. Rosenberg, C. Dahlstrand, K. Kilså, H. Ottosson, *Chem. Rev*. **2014**, *114*, 5379-5425.

[3] R. Papadakis, H. Ottosson, *Chem. Soc. Rev*. **2015**, *44*, 6472-6493.

[4] M. J. S. Dewar, *Tetrahedron Suppl.* **1966**, *22*, Supplement 8, 75-92.

[5] H. E. Zimmerman, *J. Am. Chem. Soc*. **1966**, *88*, 1564-1565.

[6] N. C. Baird, *J. Am. Chem. Soc*. **1972**, *94*, 4941-4948.

[7] H. Ottosson, *Nat. Chem.* **2012**, *4*, 969-971.

[8] (a) P. B. Karadakov, *J. Phys. Chem. A* **2008**, *112*, 7303-7309. (b) P. B. Karadakov, *J. Phys. Chem. A* **2008**, *112*, 12707-12713. (c) P. B. Karadakov, P. Hearnshaw, K. E. Horner, *J. Org. Chem.* **2016**, *81*, 11346-11352.

[9] F. Feixas, J. Vandenbussche, P. Bultinck, E. Matito, M. Solà, *Phys. Chem. Chem. Phys.* **2011**, *13*, 20690-20703.

[10] M. Estévez-Fregoso, J. Hernández-Trujillo, *Phys. Chem. Chem. Phys.* **2016**, *18*, 11792-11799.

[11] M. Kataoka, *J. Chem. Res.* **2004**, 573-574.

[12] P. Wan, E. Krogh, *J. Chem. Soc. Chem. Commun*. **1985**, 1207-1208.

[13] (a) M. Rosenberg, H. Ottosson, K. Kilså, *Phys. Chem. Chem. Phys.* **2011**, *13*, 12912-12919. (b) H. Ottosson, K. Kilså, K. Chajara, M. C. Piqueras, R. Crespo, H. Kato, D. Muthas, *Chem. Eur. J.* **2007**, *13*, 6998-7005.

[14] (a) Y. M. Sung, M-C. Yoon, J. M. Lim, H. Rath, K. Naoda, A. Osuka, D. Kim, *Nat. Chem.* **2015**, *7*, 418-422. (b) Y. M. Sung, J. Oh, W. Kim, H. Mori, A. Osuka, D. Kim, *J. Am. Chem. Soc.* **2015**, *137*, 11856-11859. (c) M. Izawa, K. Taeyeon, S-i, Ishida, T. Tanaka, T. Mori, D. Kim, A. Osuka, *Angew. Chem. Int. Ed.* **2017**, *56*, 3982-3986.

[15] Y. M. Sung, J. Oh, W-Y. Cha, W. Kim, J. M. Lim, M-C. Yoon, D. Kim, *Chem. Rev.* **2017**, *117*, 2257-2312.

[16] R. Papadakis, H. Li, J. Bergman, A. Lundstedt, K. Jorner, R. Ayub, S. Haldar, B. O. Jahn, A. Denisova, B. Zietz, R. Lindh, B. Sanyal, H. Grennberg, K. Leifer, H. Ottosson, *Nat. Commun.* **2016**, *7*, 12962-12971.

[17] R. K. Mohamed, S. Mondal, K. Jorner, T. F. Delgado, V. V. Lobodin, H. Ottosson, I. V. Alabugin, *J. Am. Chem. Soc*. **2015**, *137*, 15441-15450.

[18] L. A. Paquette, S. V. Ley, R. H. Meisinger, R. K. Russell, M. Oku, *J. Am. Chem. Soc.* **1974**, *96*, 5806-5815.

[19] V. Gogonea, P. v. R. Schleyer, P. R. Schreiner, *Angew. Chem*. **1998**, *110*, 2045-2049; *Angew. Chem. Int. Ed*. **1998**, *37*, 1945-1948.

[20] J. Zhu, K. An, P. v. R. Schleyer, *Org. Lett.* **2013**, *15*, 2442-2445.

[21] K. An, J. Zhu, *Eur. J. Org. Chem.* **2014**, *2014*, 2764-2769.

[22] (a) B. Flemmig, I. Kretzschmar, C. M. Friend, R. Hoffmann, *J. Phys. Chem. A* **2004**, *108*, 2972-2981. (b) X. Tong, G. A. Dilabio, O. J. Clarkin, R. A. Wolkow, *Nano Lett.* **2004**, *4*, 357-360. (c) A. L. Cooksy, H. F. King, W. H. Richardson, *J. Org. Chem.* **2003**, *68*, 9441-9452. (d) M. S. Samuel, H. A. Jenkins, D. W. Hughes, K. M. Baines, *Organometallics* **2003**, *22*, 1603-1611. (e) M. Newcomb, P. H. Toy, *Acc. Chem. Res*. **2000**, *33*, 449-455. (f) D. C. Nonhebel, *Chem. Soc. Rev.* **1993**, *22*, 347-359.

[23] (a) P. G. Dopico, M. G. Finn, *Tetrahedron* **1999**, *55*, 29-62. (b) W. Adam, R. Finzel, *J. Am. Chem. Soc*. **1992**, *114*, 4563-4568.

[24] (a) G. Bucher, A. A. Mahajan, M. Schmittel, *J. Org. Chem.* **2009**, *74*, 5850-5860. (b) D. A. Broyles, B. K. Carpenter, *Org. Biomol. Chem*. **2005**, *3*, 1757-1767. (c) C. Y. Gan, J. N. Lambert, *J. Chem. Soc. Perkin Trans 1* **1998**, 2363-2372. (d) C. E. Dixon, D. W. Hughes, K. M. Baines, *J. Am. Chem. Soc.* **1998**, *120*, 11049-11053. (e) P. S. Engel, K. L. Lowe, *Tetrahedron Lett*. **1994**, *35*, 2267-2270. (f) R. A. Caldwell, L. Zhou, *J. Am. Chem. Soc.* **1994**, *116*, 2271-2275. (g) P. S. Engel, D. E. Keys, *J. Am. Chem. Soc.* **1982**, *104*, 6860-6861. (h) P. J. Wagner, K.-C. Liu, Y. Noguchi, *J. Am. Chem. Soc.* **1981**, *103*, 3837-3841.

[25] M. Salamone, M. Bietti, A. Calcagni, G. Gente, *Org. Lett.* **2009**, *11*, 2453-2456.

[26] T. A. Halgren, J. D. Roberts, J. H. Horner, F. N. Martinez, C. Tronche, M. Newcomb, *J. Am. Chem. Soc.* **2000**, *122*, 2988-2994.

[27] M. Newcomb, N. Tanaka, A. Bouvier, C. Tronche, J. H. Horner, O, M. Musa, F. N. Martinez, *J. Am. Chem. Soc.* **1996**, *118*, 8505-8506.

[28] C. M. Jäger, M. Hennemann, A. Mieszała, T. Clark, *J. Org. Chem.* **2008**, *73*, 1536-1545.

[29] D. Griller, K. U. Ingold, *Acc. Chem. Res.* **1980**, *13*, 317-323.

[30] M. Newcomb, *Tetrahedron* **1993**, *49*, 1151-1176.

[31] D. W. Thomas, R. J. Brudzynski, M. L. Robin, W. L. Hase, *J. Photochem.* **1979**, *11*, 227-239.

[32] J. K. Foote, *Ph.D. Thesis.* University of California, Riverside, Calif., **1966** (University Microfilms, Ann Arbor, Michigan).

[33] R. D. S. Stevens, R. Bonneau, J. Joussot-Dubien, *J. Chem. Phys.* **1972**, *57*, 5340-5342.

[34] M. Montalti, A. Credi, L. Prodi, M. T. Gandolfi, *Handbook of Photochemistry*, CRC press, Boca Raton, 3rd Edn., **2006**.

[35] T. N. Das, K. I. Priyadarsini, *J. Chem. Soc. Faraday Trans.* **1994**, *90*, 963-968.

[36] (a) C. Tétreau, D. Lavalette, E. J. Land, F. Peradejordi, *Chem. Phys. Lett.* **1972**, *17*, 245-247. (b) F. Peradejordi, C. Tétreau, D. Lavalette, *J. Phys. Chem.* **1972**, *76*, 225-231.

[37] T. T. Talele, *J. Med. Chem.* **2016**, *59*, 8712-8756.

[38] T. M. Krygowski, M. K. Cyrański, *Tetrahedron* **1999**, *55*, 11143-11148.

[39] S. Villaume, H. A. Fogarty, H. Ottosson, *ChemPhysChem* **2008**, *9*, 257-264.

[40] S. Koseki, A. Toyota. *J.Phys. Chem. A* **1997**, 101, 5712-5718.

[41] H. Möllerstedt, M. C. Piqueras, R. Crespo, H. Ottosson, *J. Am. Chem. Soc*. **2004**, *126*, 13938-13939.

[42] L. Vannay, E. Brémond, P. de, Silva, C. Corminboeuf, *Chem. Eur. J*. **2016**, *22*, 18442-18449.

[43] R. Ayub, O. El Bakouri, K. Jorner, M. Solà, H. Ottosson, *J. Org. Chem.* **2017**, *82*, 6327-6340.

[44] T. Arai, O. Takahashi, *J. Chem. Soc. Chem. Commun.* **1995**, 1837-1838.

[45] (a) I. J. Palmer, I. N. Ragazos, F. Bernardi, M. Olivucci, M. A. Robb, *J. Am. Chem. Soc.* **1993**, *115*, 673-682. (b) B. Lasorne, M. J. Bearpark, M. A. Robb, G. A. Worth, *J. Phys.*

Chem. A **2008**, *112*, 13017-13027. (c) B. Dick, *J. Chem. Theor. Comput*. **2009**, *5*, 116-125.(d) S. Maeda, K. Ohno, K. Morokuma, *J. Chem. Theor. Comput*. **2010**, *6*, 1538-1545.

[46] S. Kallush, B. Segev, A. V. Sergeev, E. J. Heller. *J. Phys. Chem. A* **2002**, *106*, 6006-6016.

[47] M. Garavelli, F. Bernardi, A. Cembran, O. Castaño, L. M. Frutos, M. Merchán, M. Olivucci. *J. Am. Chem. Soc.* **2002**, *124*, 13770 - 13789.

[48] N. J. Turro, V. Ramamurthy, J. C. Scaiano, *Modern molecular photochemistry of organic molecules*, University Science Books, California, USA, **2010**.

[49] J. Zhao, W. Wu, J. Sun, S. Guo, *Chem. Soc. Rev.* **2013**, *42*, 5323-5351.

[50] G. Wu, M. Jr. Jones, R. Walton, P. M. Lahti, *Org. Chem.* **1998**, *63*, 5368-5371.

[51] M. Suarez. C. Devadoss, G. B. Schuster, *J. Phys. Chem*. **1993**, *97*, 9299-9303.

[52] C. Dosche, H.-G. Löhmannsröben, A. Bieser, P. I. Dosa, S. Han, M. Iwamoto, A. Schleifenbaum, K. P. C. Vollhardt, *Phys. Chem. Chem. Phys*. **2002**, *4*, 2156-2161.

[53] P. Swiderek, M. Michaud, G. Hohlneicher, L. Sanche, *Chem. Phys. Lett.* **1991**, *178*, 289-294.

[54] J. Hertzberg, B. Nickel, *Chem. Phys*. **1989**, *132*, 235-242.

[55] R. V. Bensasson, J. T. Richards, J. K. Thomas, *Chem. Phys. Lett.* **1971**, *9*, 13-16.

[56] A. T. Balaban, D. C. Oniciu, A. R. Katritzky, *Chem. Rev.* **2004**, *104*, 2777-2812.

[57] (a) P. W. Fowler, D. E. Bean, M. Seed, *J. Phys. Chem. A* **2010**, *114*, 10742-10749. (b) R. F. W. Bader, A. Streitwieser, A. Neuhaus, K. E. Laidig, P. Speers, *J. Am. Chem. Soc.* **1996**, *118*, 4959-4965.

[58] H. E. Gottlieb, V. Kotlyar, A. Nudelman, *J. Org. Chem.* **1997**, *62*, 7512-7515.

[59] P. J. Stephens, F. J. Devlin, C. F. Chabalowski, M. J. Frisch, *J. Phys. Chem*. **1994**, *98*, 11623-11627.

[60] A. D. Becke, *J. Chem. Phys*. **1993**, *98*, 1372-1377.

[61] P. C. Hariharan, J. A. Pople, *Theor. Chim. Acta.* **1973**, *28*, 213-222.

[62] (a) R. Krishnan, J. S. Binkley, R. Seeger, J. A. Pople, *J. Chem. Phys.* **1980**, *72*, 650-654. (b) A. D. McLean, G. S. Chandler, *J. Chem. Phys.* **1980**, *72*, 5639-5648.

[63] Gaussian 09, Revision D.01, Frisch, M. J. Gaussian, Inc., Wallingford CT, **2013**.

[64] (a) K. Fukui, *J. Phys. Chem.* **1970**, *74*, 4161-4163. *(b)* K. Fukui, *Acc. Chem. Res.* **1981**, *14*, 363-368.

[65] (a) T. M. Krygowski, *J. Chem. Inf. Comput. Sci.* **1993**, ***33***, 70-78. (b) T. M. Krygowski, H. Szatylowicz, O. A. Stasyuk, J. Dominikowska, M. Palusiak, *Chem. Rev.* **2014**, *114*, 6383-6422.

[66] D. Geuenich, K. Hess, F. Kohler, R. Herges, *Chem. Rev.* **2005**, *105*, 3758-3772.

[67] R. Herges, D. Geuenich, *J. Phys. Chem. A* **2001**, *105*, 3214-3220.

[68] T. A. Keith, R. F. W. Bader, *Chem. Phys. Lett.* **1993**, *210*, 223-231.

[69] F. Aquilante., *et al.* MOLCAS 8, *J. Comput. Chem.* **2016**, *37*, 506-541.

[70] B. O. Roos, P. R. Taylor, P. E. M. Siegbahn, *Chem. Phys.* **1980**, *48*, 157-173.

[71] K. Andersson, P.-Å. Malmqvist, B. O. Roos, *J. Chem. Phys.* **1992**, *96*, 1218-1226.

[72] B. O. Roos, R. Lindh, P.-Å. Malmqvist, V. Veryazov, P.-O. Widmark, *J. Phys. Chem. A.* **2004**, *108*, 2851-2858.

[73] R. S. Mulliken, *J. Chem. Phys.* **1955**, *23*, 1833-1840.

[74] A.E. Reed, R. B. Weinstock, F. Weinhold, *J. Chem. Phys.* **1985**, *83*, 735-746.

[75] R. F. W. Bader, *Chem. Rev.* **1991**, *91*, 893-928.

[76] E. D. Glendening, J. K. Badenhoop, A. E. Reed, J. E. Carpenter, J. A. Bohmann, C. M. Morales, C. R. Landis, F. Weinhold, *NBO 6.0*; Theoretical Chemistry Institute, University of Wisconsin-Madison: Madison, Wisconsin 2013.

[77] T. Lu, F. W. Chen, *J. Comput. Chem.* **2012**, *33*, 580-592.